SciMedCentral

Annals of Otolaryngology and Rhinology

Research Article

The Role of F18-FDG PET-MRI in Necrotising External Otitis Follow-Up: A Single Centre Experience

Wilhelmina L. van der Meer[1,2,3], M.D, Cristina Mitea[1,4]. M.D, Ph.D., Jérôme J. Waterval[3,5]. M.D, Ph.D., Henricus P.M. Kunst[3,5,6]. M.D, Ph.D., Felix M. Mottaghy[1,7]. M.D, Ph.D., Alida A. Postma[1,2,3]. M.D. Ph.D.

[1]*Department of Radiology & Nuclear Medicine, Maastricht University Medical Centre, The Netherlands*

[2]*School for Mental Health & Neuroscience, Maastricht University, The Netherlands*

[3]*Dutch Academic Alliance Skull Base Pathology, Maastricht University Medical Centre+, The Netherlands*

[4]*GROW-School for Oncology and Developmental Biology, Maastricht University, The Netherlands*

[5]*Department of Otorhinolaryngology and Head and Neck Surgery, Maastricht University Medical Centre, The Netherlands*

[6]*Department of Otorhinolaryngology and Head and Neck Surgery, Radboud University Medical Centre, The Netherlands*

[7]*Department of Nuclear Medicine, University Hospital RWTH, The Netherlands*

***Corresponding author**

Wilhelmina L. van der Meer, Department of Radiology & Nuclear Medicine, Maastricht University Medical Centre, The Netherlands, Tel: +31(0)43-3876543

Submitted: 13 Apr 2023

Accepted: 31 May 2023

Published: 31 May 2023

ISSN: 2379-948X

Keywords

- Necrotizing External Otitis
- Malignant External Otitis
- F18-FDG PET-MRI
- Follow-up

Abstract

Purpose of the report: Necrotizing external otitis (NEO) is a rare infectious disease arising from the external auditory canal. Follow-up of NEO is challenging, as MRI signal abnormalities can persist after adequate antibiotic treatment, and persistent/recurrent NEO can be clinically silent. The aim of this study is to investigate the clinical value of F-18-FDG PET-MR in NEO follow-up. In addition, the relation between metabolic activity responses during antibiotic treatment on F-18-FDG PET-MR was observed.

Materials and methods: This retrospective database study included patients if they had at least two F18-FDG PET-MRI scans; a baseline scan conducted at time of diagnosis/start of antibiotic treatment, and a post-treatment scan. Maximum SUV (SUVmax) on F18-FDG PET-MRI were measured by a nuclear medicine specialist, and MRI's were scored by a neuroradiologist.

Results: In total, 47 F18-FDG PET-MRI scans of 14 patients diagnosed with NEO were acquired. NEO ears show an average SUVmax on baseline scans of 7.6 ± 2.6, and significantly declined ($p<0.001$) on post-treatment scans to 2.5 ± 0.8. MRI abnormalities persisted in 86% of NEO patients. None of the patients showed clinical NEO disease recurrence.

Conclusion: The quantification of SUVmax values on F-18-FDG-PET/MRI can be used in NEO to monitor antibiotic treatment response, while the majority of NEO patients have persistent MRI abnormalities on follow-up imaging. The SUVmax of the affected ear significantly declines during antibiotic therapy, and in absence of clinical symptoms, corresponds with successful treatment.

ABBREVIATIONS

FDG: Fluorodeoxyglucose; NEO: Necrotising External Otitis; PET: Positron Emission Tomography; SUV: Standardised Uptake Value

INTRODUCTION

Necrotising External Otitis (NEO), also known as malignant external otitis, is a rare infectious disease arising from the external auditory canal. The infection can spread to the surrounding soft tissues and bone structures, and can affect muscles, cranial nerves, temporal bone structures, and the skull base. Consequently, timely and accurate diagnosis of NEO is necessary to avoid potentially life-threatening complications [1]. Patients at risk for NEO are often diabetic elderly or show an immunocompromised status. NEO can present with a variety of symptoms, ranging from otalgia, otorrhea to cranial nerve palsies [2]. *Pseudomonas aeruginosa* is the pathogen most often isolated in patients with NEO. Therefore, primary treatment commonly consists of systemic antipseudomonal antibiotics for extensive periods of time [2]. Currently, the diagnosis of NEO is based on clinical presentation, otoscopic examination, laboratory findings and radiological imaging findings through CT and/or MRI [3].

NEO can consist of involvement of osseous structures, such as the temporal and sphenoid bone, but it can also involve a range of soft tissue compartments such as the masticator space and the Para pharyngeal fat [4,5].The diagnosis is often based upon CT and MRI findings; CT to evaluate cortical destruction, and MRI for soft tissue abnormalities. However, NEO follow-up is challenging as imaging abnormalities on CT or MRI, such as bone destruction or bone marrow signal abnormalities can persist after successful antibiotic treatment [6]. In addition, persistent or recurrent NEO can be clinically silent, illustrating the need for a reliable technique to determine adequate treatment response. Alternative imaging techniques can be found in hybrid imaging options; for example F18-fluorodeoxyglucose (FDG) Positron emission tomography (PET) in combination with CT or MRI [5]. FDG-F18-PET is superior for the visualisation of tissues with high glucose metabolism (e.g. during an infectious process), therefore hybrid imaging like F18-FDG PET-MRI or F18-FDG PET-CT would allow optimal anatomical and functional imaging for the diagnosis and follow-up of hypermetabolic infectious pathologies e.g. like NEO (Figure 1).

Patterns in SUV quantification on F18-FDG PET have already been proven to give insight in the progression of different diseases and/or treatment response, which can warrant a revision in treatment plans [7,8]. A former study showed that F18-FDG PET-CT can guide clinical decision making concerning NEO antibiotic treatment duration [6], in the absence of clinical symptoms. Currently, the additional value of F-18 FDG-PET-MRI for NEO follow-up is not known.

The aim of this study is to investigate the clinical value of F-18-FDG PET-MR in NEO and the relation between antibiotic treatment and metabolic activity response on F-18-FDG PET-MR.

MATERIALS AND METHODS

This retrospective study included patients with a clinically confirmed NEO diagnosis between August 2014 and August 2022. Patients were included if they had at least two F18-FDG PET-MRI scans; a baseline scan conducted at time of diagnosis/ start of antibiotic treatment, and a post-treatment scan. Post-treatment imaging was defined as the scan acquired after the stop of antibiotic treatment and/or declaration of recovery by the clinician. Patient demographics, co-morbidities, microbiology and treatment timelines were retrieved from electronic patient records.

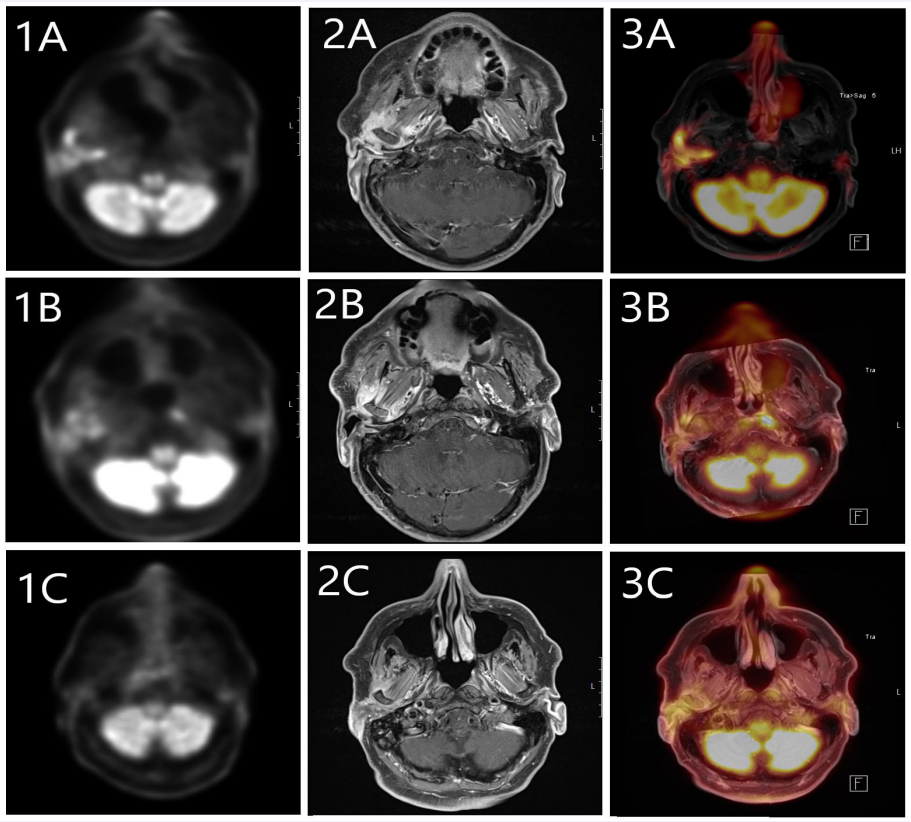

Figure 1 F18-FDG uptake during disease course. An 85-year old male patient with necrotizing external otitis due to *Pseudomonas aeruginosa* received a diagnostic FDG-PET-MR (1), a scan under antibiotic treatment (2) and after treatment (3). SUV max values showed a decline from 6.3 at diagnosis (1A), to 3.9 (2A) under antibiotic treatment and stabilized at 1.7 (3A). T1-gado sequences showed a decreased but persisting enhancement around the TMJ and infratemporal region (1B, 2B, 3B) as is also illustrated on fused images (1C,2C,3C).

Imaging Protocol

A F18-FDG PET-MRI of the skull base was performed with a dedicated PET-MRI system (Siemens Biograph). A standardised protocol for patient preparation included a minimal fasting period of 4 hours and measurements of glucose serum levels prior to intravenous injection of F18-FDG. When glucose serum levels were elevated above the 11 mmol/l cut-off value, the continuation of the imaging protocol was evaluated on a case-by-case basis by the attending nuclear physician. After injection of F18-FDG (3 MBq/kg), patients were instructed to rest in a warm room 45 min prior to imaging. Acquisition of axial T2-weighted, T2-fat saturation, T1-weighted, and post-contrast (Gadolinium 0.1 cc/kg) T1-weighted imaging with and without fat saturation were acquired. Multiplanar reconstruction, EARL reconstruction and image fusion were used as post-processing techniques.

Image Review

Reviewers were blinded for clinical data during the assessment process. Diagnostic and post-treatment PET scans were reviewed by a board certified nuclear medicine specialist (CM). NEO areas were defined as focal increased F-18-FDG uptake in combination with signal abnormalities on T1/T2 post contrast enhanced images. Manually placed regions of interest were placed in the affected and the contralateral unaffected side to measure maximum SUV (SUVmax).

MRI scans were scored by a neuroradiologist (AP). A checklist with soft tissue and osseous structures was used to score the presence of anatomical and signal abnormalities on MRI at baseline and post therapy scans. A quantified MR score was calculated as following: each abnormality on the checklist was assigned a score of 2 at baseline. In total 21 structures were scored, with a maximal score of 42 (Appendix 1). Post-therapy scans were scored as following: normal/normalization (0), improvement (1), unchanged (2), deterioration (3) for each structure on the checklist.

Appendix 1: MRI scoring

Tissue involvement	
Soft tissue	**Osseous structures**
EAC	TMJ
Masticator space	Foramen ovale
Parotid gland	Stylomastoid foramen
Retrocondylar fat	Foramen lacerum
Parapharyngeal fat	Jugular foramen
Infratemporal fat	Mastoid (lateral/caudal)
Preclival fat	Sphenoid
	Clivus
	Petroclival synchondrosis
	Petrosal apex
	Jugular fossa
Cautionary sites	
Dural enhancement	Present/absent
Intracerebral enhancement	Present/absent
Absence of flow voids	Present/absent

Tissue involvement on baseline MRI is scored as 2. Tissue involvements on post-therapy scans are scored as following: 0 (normal/normalization), 1 (improvement), 2 (unchanged), 3 (deterioration).

Statistical Analysis

Data was analysed using IBM SPSS statistics software version 28 (IBM, Armonk, New York, USA). Demographic data was analysed by descriptive statistics. Individual SUVmax course was described on case-by-case basis. The difference in SUVmax from the affected and unaffected side at baseline and post-treatment imaging, and MRI score at baseline and post-treatment scans were analysed by the Wilcoxon signed-rank test for paired samples. A significance level was set at $p < 0.05$.

RESULTS

In total, 47 F18-FDG PET-MRI scans of 14 patients diagnosed with NEO were acquired (Table 1). The majority of patients were male (79%). The mean patient age at the start of antibiotic treatment was 76.3 ± 11.8 years. Comorbidities were present in 10 patients (71%), with type II diabetes in 9 patients (64%). The most commonly isolated pathogen was *Pseudomonas aeruginosa* (71%).

F18-FDG PET-MRI

Baseline Imaging Compared to Post-Therapy Scans

The average SUVmax on baseline scans was 7.6 ± 2.6 at the affected side. The average SUVmax significantly declined ($p<0.001$) on post-treatment scans to 2.5 ± 0.8 (Figure 2). After treatment, the SUVmax between the affected and unaffected side remained significantly different ($p<0.001$). There was no significant difference of the unaffected ear at baseline (1.9 ± 0.7), and post-therapy scans (1.7 ± 0.7) ($p=0.23$). At an individual level, all patients showed a decline of SUVmax between the baseline and the post-therapy scans (Table 2).

MRI findings

All 14 patients showed abnormalities at baseline MRI scans (Table 3). Total baseline MRI scores ranged from 6-28, with a median score of 12. The most common signal abnormalities on baseline scans were of the external auditory canal (100%), infratemporal fat (100%), and retrocondylar fat (86%). After treatment 12 out of 14 patients showed persistent signal abnormalities. Total post-therapy MRI scores significantly declined with a range from 0-7, and a median score of 3 ($p<0.001$). Normalization on post-therapy MRI was seen in two patients. After treatment the most common abnormalities were of the infratemporal fat (57%), retrocondylar fat (57%), and the external auditory canal (43%).

Case-by-Case Observation

Several patients, 9 out of 14 (64%), received an interval scan to evaluate disease activity. A case-by-case observation from follow-up scans, including interval scans, showed a decreasing trend in SUVmax for 7 out of 9 patients and a rise in SUVmax

Table 1: Patient demographics

Patient	Sex	Age at start of antibiotic treatment	Co-morbidities	Affected side	Causative agent
1	M	65	Kidney Transplant (with immunosuppression)	L	P. Aeruginosa
2	F	86	Diabetes Mellitus II	L	P. Aeruginosa
3	M	85	-	R	P. Aeruginosa
4	F	81	Diabetes Mellitus II	R	P. Aeruginosa
5	M	83	-	L	C. Parapsilosis
6	M	78	Diabetes Mellitus II	R	P. Aeruginosa
7	M	84	Diabetes Mellitus II	R	No isolation of pathogen
8	M	75	-	L	P. Aeruginosa
9	M	76	Diabetes Mellitus II	L	P. Aeruginosa
10	M	41	Diabetes Mellitus II	R	P. Aeruginosa
11	M	81	-	R	P. Aeruginosa
12	M	79	Diabetes Mellitus II	R	P. Aeruginosa
13	M	65	Diabetes Mellitus II	R	Aspergillus
14	F	82	Diabetes Mellitus II + Immunosuppression for rheumatoid arthritis	R	Proteus mirabilis

Table 2: Individual MRI score and SUVmax and MRI scores at baseline and post-treatment scans

Patient	SUVmax		SUVmax		MRI score	
	Baseline		Post-treatment		Baseline	Post-treatment
	Affected ear	Unaffected ear	Affected ear	Unaffected ear		
1	5.73	1.32	1.13	0.59	26	5
2	6.93	1.97	1.3	1.18	34	7
3	6.29	1.24	3.12	1.23	14	2
4	9.48	1.45	3.73	1.65	16	5
5	10	1.52	1.87	1.47	12	3
6	2.4	1.34	2.23	2.48	8	0
7	6.91	2.17	2.17	1.78	14	6
8	11.23	1.95	3.93	3.35	10	3
9	10.45	1.79	2.3	1.07	20	4
10	3.84	3.04	2.43	2.18	16	3
11	7.49	2.65	2.66	2.15	8	1
12	10.06	1.94	2.13	1.89	12	2
13	6.26	3.29	2.94	1.09	24	0
14	8.75	1.29	3.01	1.48	20	7

Table 3: MRI imaging findings of NEO

Signal abnormalities	Diagnostic imaging N=14, (%)	Post-treatment scan (N=14), %
External auditory canal	14 (100)	6 (43)
Parotid gland	5 (36)	1 (7)
Masticator space	8 (57)	1 (7)
Retrocondylar fat infiltration	12 (86)	8 (57)
Preclival fat infiltration	3 (21)	1 (7)
Parapharyngeal fat infiltration	3 (21)	1 (7)
Infratemporal fat infiltration	14 (100)	8 (57)
TMJ	4 (29)	2 (14)
Foramen ovale	3 (21)	-
Stylomastoid foramen	9 (64)	5 (36)
Foramen lacerum	2 (14)	-
Jugular foramen	3 (21)	4 (29)
mastoid	7 (50)	4 (29)
sphenoid	1 (7)	-
Clivus	4 (29)	1 (7)
Petrosal apex	3 (21)	-
Jugular fossa	2 (14)	-
Petroclival synchodrosis	1 (7)	1 (7)
Dural enhancement	-	-
Intracranial enhancement	-	-
Flow void abnormalities	2 (14)	-

during disease course in 2 out of 7 patients (Figure 3). Patient #12 showed an increased SUVmax between baseline and interval scans. A possible explanation of this increase may be attributed to a switch from intravenous to oral antibiotics. Post-therapy scans showed a significant decrease in metabolic activity, and the patient did not show disease recurrence.

Patient #7 showed a steady decline of SUVmax in three follow-up scans. Eight weeks after the last follow-up scan, the patient underwent a post-treatment scan which showed an increase in SUVmax (from 1.7 to 3.1), attributed to a lingering infection focus. Despite this observation, the decision was made to stop antibiotic treatment for several reasons: there were no clinical arguments for progression, the glucose metabolism on the post-therapy F18-FDG PET-MRI was still significantly decreased compared to baseline, and there were no arguments for new tissue involvement on MRI. To date, the patient did not show clinical NEO recurrence for over 1 year after the last post-therapy scan.

DISCUSSION

The results of this study show that the average SUVmax

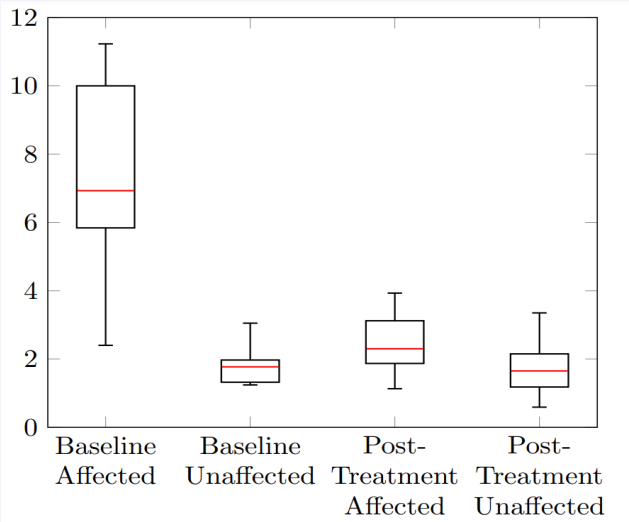

Figure 2 SUVmax boxplots for baseline and post-treatment scans.

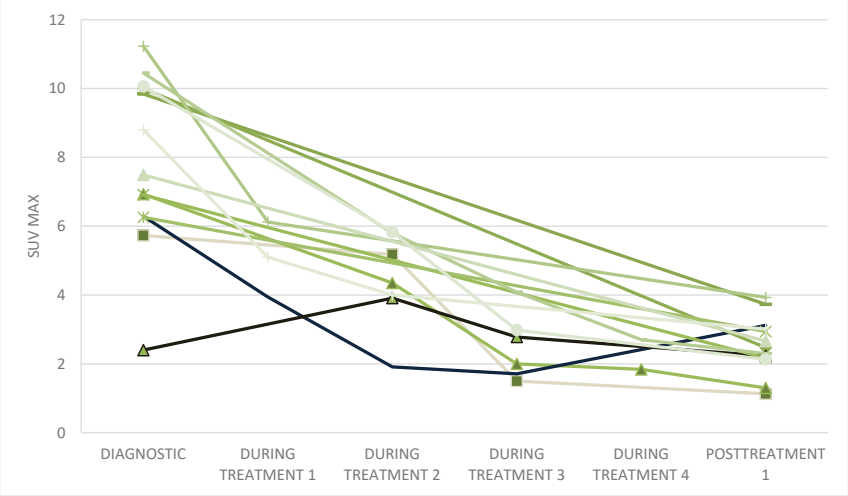

Figure 3 F18-FDG SUVmax during disease course. Each line indicates a NEO patient in which SUVmax was measured on PET-MRI during disease course. Black lines represent patients with a rise in SUVmax during disease course, and greyscale lines with a decrease SUVmax.

significantly declines after antibiotic treatment. After treatment, a metabolic difference between the affected and non-affected side remains, but does not have clinical consequences as none of the patients show disease recurrence. In addition, MRI abnormalities persist in the majority of patients (86%) after treatment. Although normalisation of MRI abnormalities was only seen in 2 patients, all patients showed a notable improvement when subsite scoring was used. For example 6 out of 14 patients showed normalisation of the infratemporal region after antibiotic treatment.

A former conducted case series showed that metabolic normalisation can be observed for F18-FDG PET-CT. The results showed that 4/8 patients had a normalisation in metabolic uptake, and 3/8 patients had strongly reduced uptake [6]. A possible explanation for metabolic normalisation on PET-CT in the aforementioned study, and absence of normalisation this current study, may be found in disease extent. Patients in the PET-CT study showed relatively limited disease as few patients showed progress beyond the external auditory canal and mastoid. For example, all patients in this current study showed involvement of the infratemporal fat.

Persistence of MRI signal abnormalities may also be correlated with disease extent. A former MRI study for NEO follow-up showed that all infra-temporal signal abnormalities remained 6 months after treatment [9], whereas 6 out of 14 patients in the current study showed normalisation after treatment. However,

none of the patients in our study showed intra-cranial extension, in contrast to a third of patients in the aforementioned study. Alternatively, the rate of metabolic and MRI normalisation may also be associated with the duration of disease. On average, there is a reported diagnostic delay of 70 days for NEO diagnosis, and subsequently adequate antibiotic therapy [10]. The mean duration from otalgia to hospitalization for the PET-CT study was 36 ± 23 days [6], whereas the average diagnostic delay for the current PET-MRI study was 9 weeks, possibly due to referral delay.

A reliable method for NEO follow-up is necessary as optimal antibiotic treatment is associated with reduced patient morbidity and mortality. FDG-PET is a promising technique as has been shown for several infectious and inflammatory diseases [8]. Previous findings of FDG-PET for skull base osteomyelitis showed a diagnostic sensitivity, specificity and accuracy of respectively 96.7%, 93.3%, and 96.1% [11]. These diagnostic values are in line with FDG-PET for peripheral osteomyelitis [12]. FDG-PET/MR has also shown to be of diagnostic value in imaging of chronic osteomyelitis in peripheral bone infections [7]. The added value of FDG-PET/MR for skull base imaging can also be expected but the current sample size is insufficient to show a possible added value.

Another limitation of this retrospective study is a possible selection bias. Clinicians who observe a mild disease course in NEO patients may not advocate follow-up by imaging, let alone by advanced hybrid imaging in the form of PET-MRI. The use of imaging methods, and recommended follow-up intervals, remain a point of discussion as there are no national NEO guidelines. The average delay of 9 weeks from symptoms to imaging with PET-MR may also reflect this lack of consensus.

It is recommended that future FDG-PET studies make use of standardised follow-up imaging intervals, as to detect early (subclinical) recurrence. Our tertiary centre included F18-FDG PET-MR as a diagnostic baseline modality. Follow-up is performed by F18-FDG-PET-MR after 6 weeks of intravenous antibiotic treatment, and additional scans are made in case of clinical deterioration, or prolonged antibiotic treatment. Due to the low incidence of NEO, and thus limited available data, a prospective multicentre study should be considered to assess SUVmax course associated with active disease and to assess whether a cut-off value can be determined.

CONCLUSION

F-18-FDG-PET/MRI is an imaging modality which can be used in NEO to monitor antibiotic treatment response. The SUVmax of the affected ear significantly declines during antibiotic therapy, and in absence of clinical symptoms, corresponds with successful treatment. None of the NEO patients showed clinical NEO recurrence, although normalisation of SUVmax was not observed.

AVAILABILITY OF DATA AND MATERIAL

The datasets generated during and/or analysed during the current study, with the exception of primary source images, are available from the corresponding author on reasonable request.

Ethical approval: Ethical approval was waived by the local Ethics Committee in view of the retrospective nature of the study and all the procedures being performed were part of routine care.

REFERENCES

1. Morales RE, Eisenman DJ, Raghavan P. Imaging necrotizing otitis externa. Semin Roentgenol. 2019; 54: 215-226.
2. Grandis JR, Branstetter BF, Yu VL. The changing face of malignant (necrotising) external otitis: Clinical, radiological, and anatomic correlations. Lancet Infect Dis. 2004; 4: 34-39.
3. Álvarez Jáñez F, Barriga LQ, Iñigo TR, Roldán Lora F. Diagnosis of skull base osteomyelitis. Radiographics. 2021; 41: 156-174.
4. Kwon BJ, Han MH, Oh SH, Song JJ, Chang KH. MRI findings and spreading patterns of necrotizing external otitis: is a poor outcome predictable? Clin Radiol. 2006; 61: 495–504.
5. Lee JE, Song JJ, Oh SH, Chang SO, Kim CH, Lee JH. Prognostic Value of Extension Patterns on Follow-up Magnetic Resonance Imaging in Patients with Necrotizing Otitis Externa. Arch Otolaryngol Head Neck Surg. 2011; 137: 688-693.
6. Stern Shavit S, Bernstine H, Sopov V, Nageris B, Hilly O. FDG-PET/CT for diagnosis and follow-up of necrotizing (malignant) external otitis. Laryngoscope. 2018; 129: 961-966.
7. Hulsen DJ, Mitea C, Arts JJ, Loeffen D, Geurts J. Diagnostic value of hybrid FDG-PET/MR imaging of chronic osteomyelitis. Eur J Hybrid Imaging. 2022 ;6: 15.
8. Glaudemans AW, Jutte PC, Cataldo MA, Victor Cassar-Pullicino , Olivier Gheysens , Olivier Borens, et al. Consensus document for the diagnosis of peripheral bone infection in adults: A joint paper by the EANM, EBJIS, and ESR (with Escmid endorsement). Eur J Nucl Med Mol Imaging. 2019; 46: 957-970.
9. Al-Noury K, Lotfy A. Computed tomography and magnetic resonance imaging findings before and after treatment of patients with malignant external otitis. Eur Arch Otorhinolaryngol. 2011; 268: 1727-1734.
10. Lau K, Scotta G, Wu K, Kabuli MA, Watson G. A review of thirty-nine patients diagnosed with necrotising otitis externa over three years: Is CT imaging for diagnosis sufficient?. Clin Otolaryngol. 2020; 45: 414-418.
11. Kulkarni SC, Padma S, Shanmuga Sundaram P. In the evaluation of patients with skull base osteomyelitis, does 18F-FDG PET CT have a role?. Nucl Med Commun. 2020; 41: 550-559.
12. Jamar F, Buscombe J, Chiti A, Paul E Christian, Dominique Delbeke, Kevin J Donohoe, et al. EANM/SNMMI guideline for 18F-FDG use in inflammation and infection. J Nucl Med. 2013; 54: 647-658.es